Proceedings of the Fifteenth International Conference on
Computational Structures Technology
Edited by: P. Iványi, J. Kruis and B.H.V. Topping
Civil-Comp Conferences, Volume 9, Paper 4.5
Civil-Comp Press, Edinburgh, United Kingdom, 2024
ISSN: 2753-3239, doi: 10.4203/ccc.9.4.5

Seismic Performance-Based Optimisation of Reinforced Concrete Dual-Systems

A. Kheradmand[1], S. Gholizadeh[1] and T. Dehghanpour Afshar[2]

[1]Department of Civil Engineering, Urmia University, Iran
[2]Faculty of Mechanical Engineering, Tabriz University, Iran

Abstract

This paper aims to optimise the initial cost of an 8-story reinforced concrete dual system using a Performance-Based Design approach. By focusing on the practical aspects of cost optimisation, this paper provides valuable insights that can be directly applied in real-world scenarios, thereby enhancing the cost-effectiveness of structures in structural engineering. This paper applies different design constraints, such as geometry, strength, and PBD constraints, in two main groups: primary and PBD constraints. Additionally, a closed-form equation is proposed to evaluate the initial cost of RC dual-system structures, using the dimensions of elements and reinforcement bars size and number as design variables. The Center of Mass Optimization algorithm, a physics-based metaheuristic, is used as an optimisation engine. A discrete section database is created to meet code-based requirements and reduce the design space.

Keywords: optimisation, reinforced concrete dual-system, performance-based design, metaheuristic, nonlinear analysis, shear wall, moment resisting frame.

1 Introduction

Structural engineers all around the world aim to find a balance between cost, safety, and efficiency, but the trial-and-error nature of structural design procedures makes it almost impossible to try all possible structure samples to achieve this goal properly;

hence, structural optimisation methods try to redefine the path to find the balance of cost and safety in engineering. Nowadays, among different methodologies for earthquake-resistant structure design, performance-based design (PBD) [1] is a trustworthy and effective approach for developing buildings that can withstand seismic activity over various intensities. In recent years, performance-based design optimisation (PBDO) methodologies have been developed to design cost-effective, safe structures. A reinforced concrete (RC) dual system is a structural system that efficiently transfers lateral loads to the supports by combining structural walls with moment-resisting frames. This structural system is mainly used in mid-to high-rise structures.

Saka [2] presented a method for optimising multistorey RC structures with shear walls, considering ultimate axial load, story drift, ultimate moment, and minimum size as the design constraints. Razavi and Gholizadeh [3] studied the PBDO of RC frames, considering the life-cycle cost of the structure as the objective function. Hoseini Vaez and Gomi [4] optimised the RC shear walls bar layout and boundary element dimensions using different algorithms. Lou et al. [4] suggested a framework for optimising high-rise RC shear wall structures and optimised them using linear static procedures. Kaveh and Zakian [5] optimised the RC dual-systems using equivalent static procedures. This paper aims to fill a research gap regarding the seismic PBDO of RC dual systems.

2 Methods

2.1 Optimization Algorithm

In recent decades, a wide range of metaheuristic algorithms have been developed for structural optimisation. The algorithms are inspired by different aspects of nature, such as evolutionary theory, biology, and physics. They are superior to classic gradient-based methods in dealing with complex optimisation problems [6].

The Center of Mass Optimization (CMO) algorithm is a physics-based metaheuristic algorithm developed by Gholizadeh and Ebadijalal [7]. The basic idea behind the CMO is that mass distribution must be centred in space. Recent research indicates that CMO surpasses certain metaheuristics in dealing with benchmark sizing optimisation challenges for truss structures and seismic performance-based design optimisation of steel moment-resisting frames. Furthermore, the CMO algorithm contains a powerful mechanism for efficiently transitioning between exploration and exploitation during its search process. This feature makes CMO particularly well-suited for addressing complicated optimisation problems. Thus, this work utilises the CMO algorithm to optimise the mentioned structure.

2.2 Design Constraints

Satisfying three types of design constraints encompassing geometric, strength and PBD constraints is necessary to ensure the feasibility of generated structures throughout the optimisation process of the RC dual systems. The geometric constraints, denoted by g_{GEO}, indicate that in each beam-column joint, the dimensions as width, height, and web thickness (for walls), the number and diameter of steel

reinforcements in the bottom column and walls must be matched to or more than those in the top column and wall, respectively.
For columns:

$$g_{GEO,C} = \begin{cases} \frac{b_{c,T}}{b_{c,B}} - 1 \leq 0 \\ \frac{h_{c,T}}{h_{c,B}} - 1 \leq 0 \\ \frac{n_{c,T}}{n_{c,B}} - 1 \leq 0 \\ \frac{d_{c,T}}{d_{c,B}} - 1 \leq 0 \end{cases} \quad (1)$$

For walls:

$$g_{GEO,W} = \begin{cases} \frac{b_{w,T}}{b_{w,B}} - 1 \leq 0 \\ \frac{h_{w,T}}{h_{w,B}} - 1 \leq 0 \\ \frac{n_{w,T}}{n_{w,B}} - 1 \leq 0 \\ \frac{d_{w,T}}{d_{w,B}} - 1 \leq 0 \\ \frac{t_{w,T}}{t_{w,B}} - 1 \leq 0 \end{cases} \quad (2)$$

in which $g_{GEO,C}$ and $g_{GEO,W}$ are geometry constraints of columns and walls; $b_{c,T}$, $h_{c,T}$, $n_{c,T}$, $d_{c,T}$, $b_{c,B}$, $h_{c,B}$, $n_{c,B}$, and $d_{c,B}$ are the width, height, and the number and diameter of reinforcement bars of the top column and bottom column correspondingly. Also $b_{w,T}$, $h_{w,T}$, $n_{w,T}$, $d_{w,T}$, $t_{w,T}$, $b_{w,B}$, $h_{w,B}$, $n_{w,B}$, $d_{w,T}$, and $t_{w,B}$ are boundary element width, height, number and diameter of reinforcement bars, and wall web thickness, respectively.

According to the ACI 318–19 [8] design code, demand-to-capacity ratio for each structural element must be less than one for non-seismic gravity loads as the strength constraints (g_{STR}). The selected design should be modified if the geometry and strength criteria are not met.
For columns:

$$g_{STR,C} = \begin{cases} \frac{M_{Max,C}}{\varphi M_{n,C}} - 1 \leq 0 \\ \frac{N_{Max,C}}{\varphi N_{n,C}} - 1 \leq 0 \\ \frac{V_{Max,C}}{\varphi V_{n,C}} - 1 \leq 0 \end{cases} \quad (3)$$

For beams:

$$g_{STR,B} = \begin{cases} \frac{M_{Max,B}}{\varphi M_{n,B}} - 1 \leq 0 \\ \frac{N_{Max,B}}{\varphi N_{n,B}} - 1 \leq 0 \\ \frac{V_{Max,B}}{\varphi V_{n,B}} - 1 \leq 0 \end{cases} \quad (4)$$

For walls:

$$g_{STR,W} = \begin{cases} \frac{M_{Max,W}}{\varphi M_{n,W}} - 1 \leq 0 \\ \frac{N_{Max,W}}{\varphi N_{n,W}} - 1 \leq 0 \\ \frac{V_{Max,W}}{\varphi V_{n,W}} - 1 \leq 0 \end{cases} \quad (5)$$

where $c_{STR,C}$, $c_{STR,B}$, and $c_{STR,W}$ are strength constraints of columns, beams, and walls. $M_{Max,C}$, $N_{Max,C}$, $V_{Max,C}$, $M_{Max,B}$, $N_{Max,B}$, $V_{Max,B}$, $M_{Max,W}$, $N_{Max,W}$, and $V_{Max,W}$ are maximum bending moment, axial force, and shear demand of columns, beams, and walls. $M_{n,C}$, $N_{n,C}$, $V_{n,C}$, $M_{n,B}$, $N_{n,B}$, $V_{n,B}$, $M_{n,W}$, $N_{n,W}$, and $V_{n,W}$ are nominal bending moment, axial, and shear capacity of column, beam, and wall elements. Variable φ indicates the strength reduction factor for each type of element and action based on ACI 318-19 [8] provisions.

If the geometric and strength constraints are satisfied, a nonlinear static analysis with the displacement coefficient approach [9] utilised to check the PBD constraints. To achieve this, the seismic nonlinear responses of the structure should be evaluated at three performance levels. Therefore, the present study considers three seismic hazard levels represented by 50%/50y, 10%/50y, and 2%/50y, corresponding to a 50%, 10%, and 2% probability of exceedance in 50 years, respectively. The site's response spectrum was determined using the ASCE hazard tool data, as addressed in ASCE7-22 [10]. The considered parameters are S_{m1}=0.76g and S_{ms}=2.13g, resulting in T_0=0.071s and Ts=0.357s.

The maximum inter-story drift (ISD) ratios at each performance level (ISD^{IO}, ISD^{LS}, and ISD^{CP}) must not exceed the allowable values of $ISD^{IO}_{all.}$= 0.5%, $ISD^{LS}_{all.}$= 1%, and $ISD^{CP}_{all.}$= 2%, as stated in FEMA-356 [9]. The constraint for inter-story drift (g_{ISD}) can be expressed as follows:

$$g_{ISD}: \begin{cases} g^{IO}_{ISD} = \frac{ISD^{IO}}{ISD^{IO}_{all.}} - 1.0 \leq 0 \\ g^{LS}_{ISD} = \frac{ISD^{LS}}{ISD^{LS}_{all.}} - 1.0 \leq 0 \\ g^{CP}_{ISD} = \frac{ISD^{CP}}{ISD^{CP}_{all.}} - 1.0 \leq 0 \end{cases} \quad (6)$$

PBD necessitates an assessment of the plastic hinge rotation (PHR) capacities of the beams, columns, and walls in RC Dual system members at each performance level. So, the plastic hinge rotation constraint (g_{PHR}) can be formulated as follows:
For columns:

$$g_{PHR,C}: \begin{cases} \frac{PHR_C^{IO}}{PHR_{all,C}^{IO}} - 1.0 \leq 0 \\ \frac{PHR_C^{LS}}{PHR_{all,C}^{LS}} - 1.0 \leq 0 \\ \frac{PHR_C^{CP}}{PHR_{all,C}^{CP}} - 1.0 \leq 0 \end{cases} \quad (7)$$

For beams:

$$g_{PHR,B}: \begin{cases} \frac{PHR_B^{IO}}{PHR_{all,B}^{IO}} - 1.0 \leq 0 \\ \frac{PHR_B^{LS}}{PHR_{all,B}^{LS}} - 1.0 \leq 0 \\ \frac{PHR_B^{CP}}{PHR_{all,B}^{CP}} - 1.0 \leq 0 \end{cases} \quad (8)$$

For walls:

$$g_{PHR,W}: \begin{cases} \frac{PHR_W^{IO}}{PHR_{all,W}^{IO}} - 1.0 \leq 0 \\ \frac{PHR_W^{LS}}{PHR_{all,W}^{LS}} - 1.0 \leq 0 \\ \frac{PHR_W^{CP}}{PHR_{all,W}^{CP}} - 1.0 \leq 0 \end{cases} \quad (9)$$

where $g_{PHR,C}$, $g_{PHR,B}$, and $g_{PHR,W}$ are plastic hinge rotation constraints of columns, beams, and walls, respectively. The plastic hinge rotation for each component (beam, column, and wall) at IO, LS, and CP performance levels are denoted respectively by $PHR_{B,}^{IO}$, $PHR_{B,}^{LS}$, PHR_B^{CP}, PHR_C^{IO}, PHR_C^{LS}, PHR_C^{CP}, PHR_W^{IO}, PHR_W^{LS}, PHR_W^{CP} and their allowable values are represented by $PHR_{all,B}^{IO}$, $PHR_{all,B}^{LS}$, $PHR_{all,B}^{CP}$, $PHR_{all,C}^{IO}$, $PHR_{all,C}^{LS}$, $PHR_{all,C}^{CP}$, $PHR_{all,W}^{IO}$, $PHR_{all,W}^{LS}$ and $PHR_{all,W}^{CP}$ based on ASCE 41-23 [11] provisions.

According to the ACI 318–19 [8] provisions, hinging in the beam-column joint must be initiated in beam region. Therefore, the strong-column-weak-beam criterion (g_{SCWB}) is considered in each beam-column joint as follows:

$$g_{SCWB} = 1.2 \times \left(\frac{\sum M_{nB}}{\sum M_{nC}}\right) - 1 \leq 0 \quad (10)$$

where $\sum M_{nB}$ and $\sum M_{nC}$ are the sum of the nominal flexural strengths of the beams and columns connected to the joint, respectively.

2.3 Cost Function

The variables of the design optimisation of the RC dual system are the cross-section details of columns, beams, and walls. By using predetermined databases of code-compliant cross-sections for columns, beams, and walls, the computational cost of the optimisation process remarkably decreases. This study uses three sets of section databases for the columns, beams, and walls. Table 1 gives the database of columns in which the width (b) and height (h) of the sections are assumed to be equal and vary from 0.4 m to 1.1 m. The bar's diameter is 25 mm for section height and width less than 0.9 m and 32 mm for height and width more than or equal to 0.9 m.

The database of beam sections is shown in Table 2. The variables are width (b), height (h), and the number of reinforcement bars at the top and bottom of sections. In which, b varies between 0.35 m and 0.4 m with an increment of 0.05 m, and h differs between 0.6 m and 0.7 m with an increment of 0.05 m. For all sections, the reinforcement bar diameter is 22 mm.

	Dim.		reinforcement Bar	
No.	b (m)	h (m)	number	Dia.
1	0.4	0.4	4	D25
2	0.4	0.4	6	D25
3	0.4	0.4	8	D25
…	…	…	…	…
44	1.1	1.1	24	D32
45	1.1	1.1	26	D32
46	1.1	1.1	28	D32

Table 1: Database of columns.

The wall's section database is given in Table 3, and the variables are boundary element width (bf) and height (tf), web thickness (tw), distance of the vertical and horizontal shear bars (Ssh), and the number of reinforcement bars at each boundary element. In this table, bf and tf are assumed to be equal and vary between 0.3 m and 0.9 m with an increment of 0.1 m. For bf and tf less than 0.9 m, tw is considered 0.3 m; for bf and tf more than 0.9 m, tw is regarded as 0.4 m. Also, a diameter of 22 mm was used for all sections' boundary element reinforcement bars, and Ssh was 0.35 m for all sections. The web vertical and horizontal shear bars' diameter is 16 mm. Figure 1 depicts the cross sections of walls, beams, and columns.

	Dim.		number of reinforcement Bar D22	
No.	b (m)	h (m)	Top	Bot
1	0.35	0.6	5	3
2	0.35	0.6	4	4
3	0.35	0.6	3	5
…	…	…	…	…
59	0.4	0.7	10	8
60	0.4	0.7	9	9
61	0.4	0.7	8	10
62	0.4	0.7	10	10

Table 2: Database of beams.

No.	Dim.			number of reinforcement Bar D22	
	bf & tf	tw	Ssh	Nrl	Nud
1	300	300	350	2	6
2	400	300	350	2	6
3	400	300	350	4	8
…	…	…	…	…	…
25	900	400	350	20	24
26	900	400	350	22	26
27	900	400	350	24	28

Table 3: Database of walls.

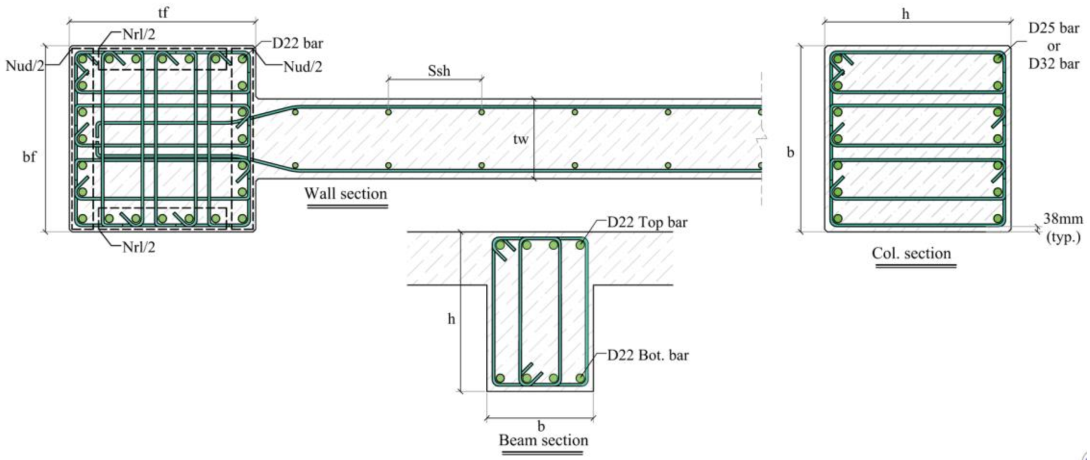

Figure 1: Cross sections of walls, beams, and columns.

The initial cost can be calculated by adding together the expenses for steel bars, concrete, and the framework of columns, beams, and walls as follows:

$$C_{Column} = \sum_{i=1}^{nc}\left[C_C b_{c,i} h_{c,i} + C_S A_{s,c,i} + 2C_F\left(b_{c,i} + h_{c,i}\right)\right] H_{i,c} \quad (11)$$

$$C_{Beam} = \sum_{j=1}^{nb}\left[C_C b_{b,j} h_{b,j} + C_S A_{s,b,j} + C_F\left(b_{b,j} + 2h_{b,j}\right)\right] L_{j,b} \quad (12)$$

$$C_{Wall} = \sum_{k=1}^{nw}\left[C_C\left(2b_{f,k}t_{f,k} + h_{w,k}t_{w,k}\right) + C_S\left(2A_{sf,k} + A_{sw,k}\right) + C_F\left(4\left(b_{f,k} + t_{f,k}\right) + 2h_{w,k} - 2t_{w,k}\right)\right] H_{k,w} \quad (13)$$

$$C_I = C_{Column} + C_{Beam} + C_{Wall} \quad (14)$$

where C_{Column}, C_{Beam}, and C_{Wall} represent the cost of columns, beams, and walls, respectively; C_I represents the initial cost of the RC dual-system; $b_{c,i}$, $h_{c,i}$, $A_{s,c,i}$, and $H_{i,c}$ represent the width, height, area of reinforcement bars, and height of the ith column, respectively; similarly $b_{b,j}$, $h_{b,j}$, $A_{s,b,j}$, and $L_{j,b}$ represent the width, height, area of reinforcement bars, and length of the jth beam, respectively; $b_{f,k}$, $t_{f,k}$, $h_{w,k}$, $t_{w,k}$, $A_{sf,k}$, $A_{sw,k}$,and $H_{k,w}$ represent the boundary element width and height, length of the shear wall's web, wall's web thickness, area of boundary element reinforcement bars, area of wall's web reinforcement bars, and height of the kth wall, respectively; nc, nb, and nw represent the numbers of columns, beams, and walls, respectively; The unit costs of concrete, reinforcement, and framework are denoted by C_C, C_S, and C_F, respectively, with values of 105 $/m^3, 7065 $/m^3, and 92 $/m^2, respectively[3].

2.4 Modelling Details

Figure 2 shows the archetype structure plan, elevation, and section views. The lateral-load-resisting components consist of two sets of three-bay frames positioned at the structure perimeter (A and F axis) and two sets of RC walls situated toward the centre of the building (E and B axis) in each direction.

OpenSees [12] platform is used to conduct nonlinear static analysis of the lateral-force-resisting system. This paper employs a two-dimensional model, neglecting torsion and incorporating symmetry. The model has a single three-bay frame and a single wall, as shown in Figure 3.

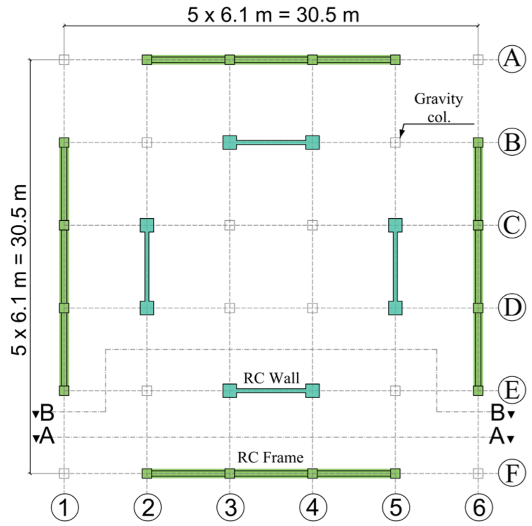

(a)

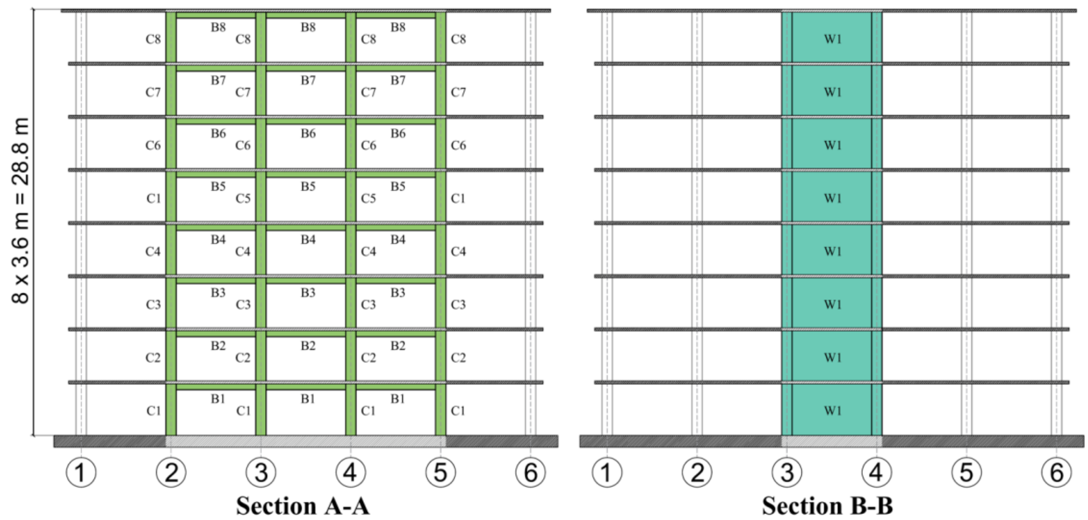

(b)

Figure 2: Archetype structure (a) plan and (b) elevation views.

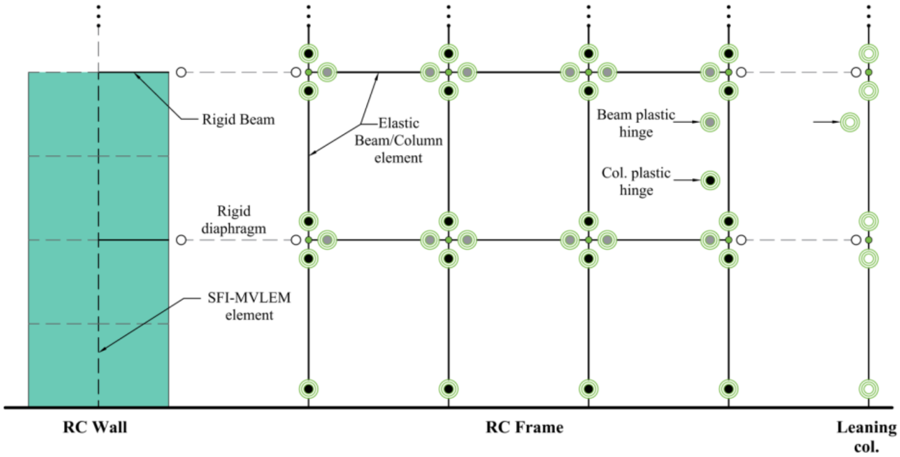

Figure 3: Analytical model.

The gravity system is not included in the model according to the ASCE 7-22 [10] requirements; hence, the leaning-column concept has been utilised to consider the P-delta effect, as shown in Figure 3. The tributary mass is allocated to the element nodes at each story level along the axes of the wall and columns.

The gravity load, consisting of dead and live loads, is assigned based on the corresponding tributary areas. RC frame elements (i.e., beams and columns) are modelled using elastic beam-column elements by assuming the location of plastic hinges at the faces of beam-column joints, as shown in Figure 3. The behaviour of hinges is simulated using the moment-rotation hysteretic model proposed by Lignos and Krawinkler [13], with modelling parameters adopted according to beam and column flexural capacities and backbone relationships proposed by Haselton et al. [14]. The behaviour of RC walls was simulated using the wall model proposed by Kolozvari et al. [15] that incorporates the interaction between axial-flexural and shear behaviour under cyclic loading conditions. Concrete compressive strength of $f_c' = 35$ MPa and reinforcing steel (longitudinal and transversal) with yield strength of $f_y = 415$ MPa is assumed. A uniformly distributed dead load of 7.18 kN/m^2 and live load of 1.91 kN/ m^2 as per ASCE7-22 [10] are used.

2.5 PBDO Formulation

In this work, the design variables vector is defined as follows:

$$X = \{X_{Column} \quad X_{Beam} \quad X_{Wall}\} \tag{15}$$

where X_{Column}, X_{Beam}, and X_{Wall} represent variables regarding columns, beams, and walls, respectively. As the beams, columns, and walls of the RC dual system are divided into several groups, X_{Column}, X_{Beam}, and X_{Wall} are defined as follows:

$$X_{Column} = \{C_{g1} \;\; C_{g2} \;\ldots\; C_{gnc}\} \tag{16}$$
$$X_{Beam} = \{B_{g1} \;\; B_{g2} \ldots B_{gnb}\} \tag{17}$$
$$X_{Wall} = \{W_{g1} \;\; W_{g2} \ldots W_{gnw}\} \tag{18}$$

Where nc, nb, and nw represent the number of column, beam, and wall groups, respectively; C_{g1} to C_{gnc}, B_{g1} to B_{gnb}, and W_{g1} to W_{gnw} are the design variables of columns, beams, and walls, respectively.

The PBDO problem of RC dual systems can be stated as follows:

$$\text{minimize: } C_I(X) \tag{19}$$

$$\text{subject to:} \begin{cases} g_{GEO} \leq 0 \\ g_{STR} \leq 0 \\ g_{ISD} \leq 0 \\ g_{PHR} \leq 0 \\ g_{SCWB} \leq 0 \end{cases} \tag{20}$$

If a candidate structure violates geometric and strength constraints, it will be revised; otherwise, a nonlinear static analysis will be conducted to evaluate the seismic responses of the structure to check the PBD constraints.

This study utilises the exterior penalty function technique (EPFM) [16] to handle the design constraints of the PBDO problem of the RC dual systems. In this case, the pseudo-unconstrained objective function to be minimised, is stated as follows:

$$\emptyset = C_I(X).\left(1 + rp.\sum_{k=1}^{n}\left(g_k(X)\right)^2\right) \tag{21}$$

where $\emptyset$ is the pseudo-unconstrained objective function; rp is the penalty parameter, and n is the number of design constraints.

3 Numerical Results

Table 4 shows the best results obtained from 40 independent optimisation runs of an 8-story RC dual system. The population size and the maximum iterations are 100 and 200, respectively.

Element		Dim. (m)		Bars	
type	group	b	h	Top	Bot.
Beam	B1	0.35	0.6	3D22	5D22
	B2	0.35	0.6	4D22	6D22
	B3	0.35	0.6	5D22	3D22
	B4	0.4	0.7	10D22	8D22
	B5	0.35	0.65	5D22	3D22
	B6	0.35	0.65	3D22	3D22
	B7	0.35	0.6	4D22	6D22
	B8	0.35	0.65	5D22	3D22
Column	C1	0.6	0.6	16D25	
	C2	0.6	0.6	16D25	
	C3	0.6	0.6	14D25	
	C4	0.6	0.6	14D25	
	C5	0.6	0.6	14D25	
	C6	0.6	0.6	12D25	
	C7	0.6	0.6	12D25	
	C8	0.6	0.6	12D25	
wall		bf & tf	tw	Ssh	Nrl	Nud
	W1	0.4	0.3	0.35	4D22	8D22
Optimal initial cost: $111790.90					
Computational cost: 6481 pushover analysis (29520 sec)					

Table 4: The best solution details.

The initial costs of all the optimal designs are displayed in Figure 4. The average of the optimal costs is $117181.08, and the standard deviation (STD) is $3421.07.

Figure 5 shows the convergence curves of all the optimisation runs, including the best and mean convergence curves.

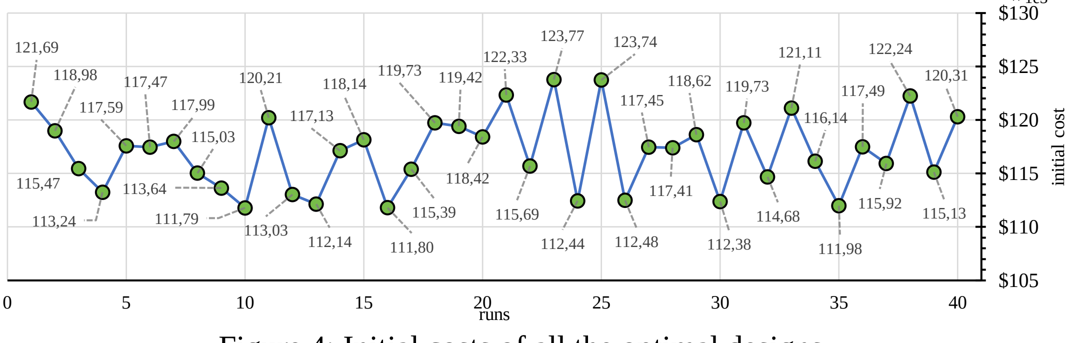

Figure 4: Initial costs of all the optimal designs.

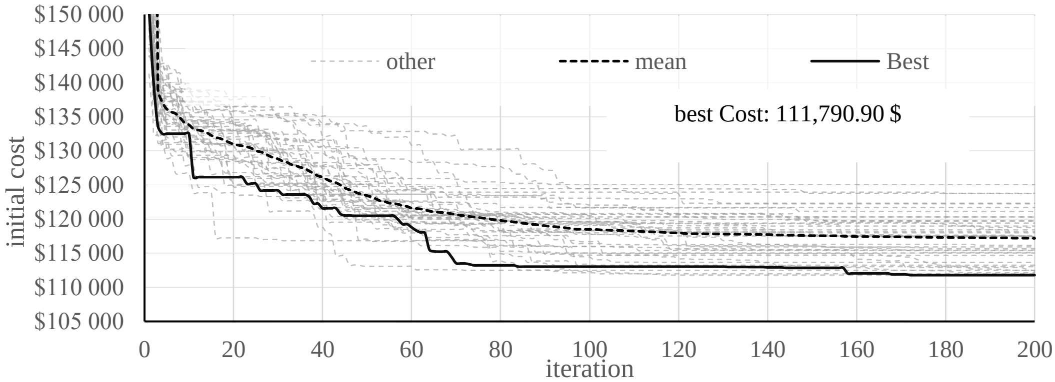

Figure 5: Convergence curves of all the optimisation runs.

For the best design, Figure 6(a) shows the inter-story drift ratio profile at three performance levels, Figure 6(b) shows the maximum plastic hinge rotation demand-capacity-ratio (DCR) for all the element groups, Figure 6(c) shows push-over curves and Figure 6(d) shows the SCWB ratio of each beam-column joint. It can be observed that the inter-story drift ratio constraint at the LS performance level dominates the design.

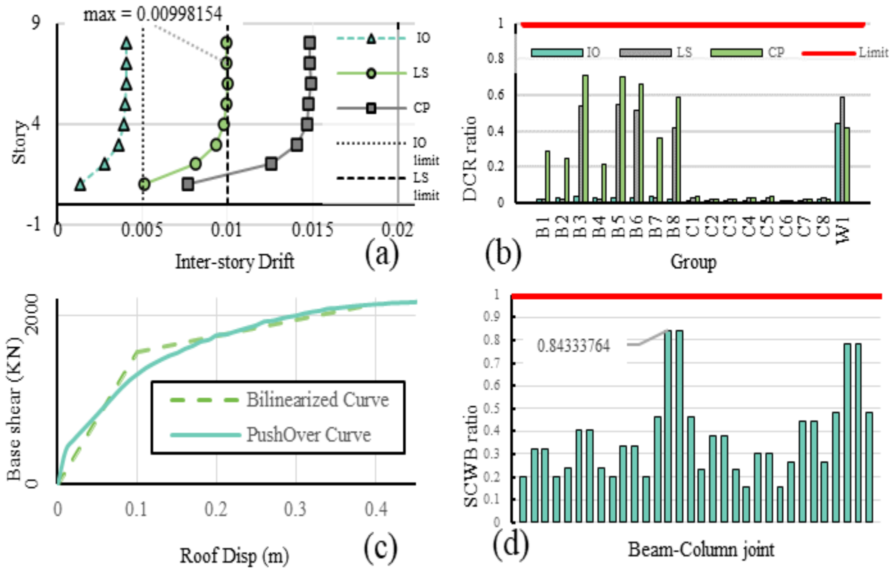

Figure 6: Seismic responses of the best solution.

4 Conclusions and Contributions

This study is devoted to optimising reinforced concrete dual systems in the framework of seismic performance-based design. An efficient metaheuristic, the centre of mass optimisation algorithm, is utilised to achieve the optimisation task.

An 8-story reinforced concrete dual-system is presented as an illustrative example, and the main findings of this study are summarised as follows:

i. The active constraint that dominates the optimum design is the inter-story drift ratio at the LS performance level, with a maximum value of 0.00998154, which is 99.8% of the allowable value.

ii. The plastic hinges are mainly concentrated in beams and walls, with columns not exceeding 10% of their capacity at each performance level.
iii. The second active constraint is the strong-column-weak-beam constraint with a maximum ratio of 0.8433.

References

[1] A.T. Council, U.S.F.E.M. Agency, "ATC 63 (FEMA P-695): Quantification of Building Seismic Performance Factors ", U.S. Department of Homeland Security, FEMA, Redwood City, California, 2009.

[2] M.P. Saka, "Optimum Design of Multistorey Structures with Shear Walls", Computers & Structures, 44, 925-936, 1992.

[3] N. Razavi, S. Gholizadeh, "Seismic Collapse Safety Analysis of Performance-Based Optimally Designed Reinforced Concrete Frames Considering Life-cycle Cost", Journal of Building Engineering, 44, 103430-103444, 2021.

[4] H.P. Lou, J. Ye, F.L. Jin, B.Q. Gao, Y.Y. Wan, G. Quan, "A Practical Shear Wall Layout Optimization Framework for the Design of High-rise Buildings", Structures, 34, 3172-3195, 2021.

[5] A. Kaveh, P. Zakian, "Optimal Seismic Design of Reinforced Concrete Shear Wall-Frame Structures", KSCE Journal of Civil Engineering, 18, 2181-2190, 2014.

[6] S. Mirjalili, S.M. Mirjalili, A. Lewis, "Grey Wolf Optimizer", Advances in Engineering Software, 69, 46-61, 2014.

[7] S. Gholizadeh, M. Ebadijalal, "Performance Based Discrete Topology Optimization of Steel braced Frames by a New Metaheuristic", Advances in Engineering Software, 123, 77-92, 2018.

[8] A.C. 318, "ACI 318-19(22): Building Code Requirements for Structural Concrete and Commentary", American Concrete Institute, Farmington Hills, 2019.

[9] F.E. Agency, "FEMA 356: Prestandard and Commentary for the Seismic Rehabilitation of Buildings", CreateSpace Independent Publishing Platform, Washington, D.C., 2013.

[10] A.S.o.C. Engineers, "ASCE 7-22: Minimum Design Loads and Associated Criteria for Buildings and Other Structures", American Society of Civil Engineers, Reston, Virginia, 2022.

[11] S.E. Institute, A.S.o.C. Engineers, "ASCE/SEI 41-23: Seismic Evaluation and Retrofit of Existing Buildings", American Society of Civil Engineers, Reston, Virginia, 2023.

[12] F. McKenna, "OpenSees: a Framework for Earthquake Engineering Simulation", Computing in Science & Engineering, 13, 58-66, 2011.

[13] D.G. Lignos, H. Krawinkler, "Deterioration Modeling of Steel Components in Support of Collapse Prediction of Steel Moment Frames Under Earthquake Loading", Journal of Structural Engineering, 137, 1291-1302, 2011.

[14] C.B. Haselton, A.B. Liel, S.C. Taylor-Lange, G.G. Deierlein, "Calibration of Model to Simulate Response of Reinforced Concrete Beam-Columns to Collapse", ACI Structural Journal, 113, 1141-1152, 2016.

[15] K. Kolozvari, K. Orakcal, J.W. Wallace, "Modeling of Cyclic Shear-Flexure Interaction in Reinforced Concrete Structural Walls. I: Theory", Journal of Structural Engineering, 141, 401-413, 2015.

[16] G.N. Vanderplaats, "Numerical Optimization Techniques for Engineering Design: with Applications", McGraw-Hill, New York, 1984.